# Chapter 4

## CLASSICAL, REFINED, ZIG-ZAG AND LAYER-WISE MODELS FOR LAMINATED STRUCTURES

Erasmo Carrera and Maria Cinefra
*Aerospace Department, Politecnico di Torino,*
*Corso Duca degli Abruzzi 24, 10129 Torino, Italy*

**Abstract**

This chapter overviews classical and advanced theories for laminated plates and shell structures. Findings from existing historical reviews are used to confirm that the advanced theories can be grouped and referred to as: Lekhnitskii multilayered theories, Ambartsumian multilayered theories, and Reissner multilayered theories. The unified formulation proposed by the first author, which is known as CUF (Carrera's unified formulation), is used to make numerical assessments of various laminated plate/shell theories. The chapter ends by giving details of a recent reliable finite element formulation for laminated shell analysis. It is embedded in the CUF framework and it leads to the classical, zig-zag, and layer-wise models as particular cases. Numerical mechanisms such as shear and membrane locking are contrasted by developing an appropriate choice of shape functions and mixed assumed shear strain techniques.

### 4.1 Introduction

Two–dimensional (2D) modeling of multilayered plates and shells requires appropriate theories. The discontinuity of physical/mechanical properties in the thickness direction makes theories that were originally developed for one-layered structures inadequate, such as the Cauchy–Poisson–Kirchhoff–Love thin plate/shell theories [1–4], or the Reissner and Mindlin [5, 6] first-order shear deformation theory (FSDT) as well as higher-order models such as that by Hildebrand, Reissner, and Thomas [7]. These theories are in fact not able to reproduce piecewise continuous displacement and transverse stress fields in the

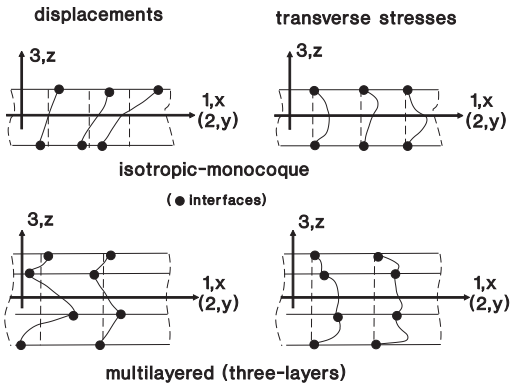


Fig. 4.1. $C_z^0$-requirements. Single-layered and three-layered structures.

thickness direction, which are usually experienced by multilayered structures. These two fields are often described in the literature as *zig-zag effects* and *interlaminar continuity,* respectively (see also the three-dimensional solutions reported by Pagano [8]). In [9] these two effects have been summarized using the acronym $C_z^0$-requirements, that is displacements and transverse stresses must be $C^0$-continuous functions in the $z$-thickness directions. A qualitative comparison of displacement and stress fields in a one–layered and a multilayered structure are depicted in Fig. 4.1. This picture clearly shows that theories designed for one-layer structures are inappropriate to analyze multilayered ones.

A number of refinements of classical models as well as theories designed for multilayered structures have been proposed in the literature over the last four decades. Due to the form of displacement fields (see Fig. 4.1), the latter are often referred to as "zig-zag" theories. For a complete review of this topic, readers who are interested can refer to the many available survey articles on beams, plates, and shells. Among these, excellent reviews are quoted in the articles by Ambartsumian [10], Librescu and Reddy [11], Grigolyuk and Kulikov [12], Kapania and Raciti [13], Kapania [14], Noor and co-authors [15–17], Reddy and Robbins [18], Carrera [19], as well as in the books by Librescu [20] and Reddy [21]. These articles review theories that deal with layer-wise models (LWMs) and equivalent single-layer models (ESLMs). Following Reddy [21], it is intended that the number

of displacement variables is kept independent of the number of constitutive layers in the ESLM, while the same variables are independent in each layer for LWM cases.

Although these review works are excellent, in the authors' opinion, there still exists the need for a historical review with the aim of giving clear answers to the following questions:

(1) Who first presented a zig-zag theory for a multilayered structure?
(2) How many different and independent ESL zig-zag theories have been proposed in open literature?
(3) Who first proposed the theories for question 2?
(4) Are the original works well recognized and mentioned correctly in subsequent articles?
(5) What are the main differences among the available approaches to multilayered structures?

The answers to these five points could be extremely useful to analysts of layered structures. Furthermore, it will give an insight into early and, equally very interesting, ideas and methods such as those by Lekhnitskii [22], which could be extended and applied to further problems. In particular, answers to questions 1 and 3 could establish a sort of historical justice, therefore permitting us to give to "Caesar what belongs to Caesar and to God what belongs to God."

This chapter is therefore a historical review of "zig-zag" theories, which can describe what have previously been called $C_z^0$-requirements, in view of questions 1–5. These topics have already been documented in the historical note by the first author [23]. The findings in that paper are reconsidered in the first part of this chapter.

The present chapter considers mostly ESLMs. For the sake of completeness, a few comments on layer-wise cases are given in a separate section. A further limitation of the present chapter is that it is restricted to axiomatic type-approaches. The three multilayered theories discussed introduce initial assumptions: stress function forms were assumed by Lekhnitskii, transverse shear stress fields were assumed by Ambartsumian, while both displacements and transverse shear stresses were assumed in the framework of the mixed theorem proposed by Reissner. Therefore, those works which are based on asymptotic expansion such as those in [24–26] have not been discussed in the present chapter.

The latter part of this chapter considers the development of a refined shell finite element formulation, which is based on Carrera's unified formulation (CUF) [27, 28].

The most common mathematical models used to describe shell structures may be classified into two classes according to their different physical assumptions. The Koiter model [29] is based on the Kirchhoff hypothesis. The Naghdi model [30] is based on the Reissner–Mindlin assumptions, which take into account transverse shear deformation. It is known that when a finite element method is used to discretize a physical model, numerical *locking* may arise from hidden constraints that are not well represented in the finite element approximation. In the Naghdi model both transverse shear and membrane constraints appear as the shell thickness becomes very small, thus locking may arise. The most common approaches proposed to overcome the locking phenomenon are the standard displacement formulation with higher-order elements [31, 32] or techniques of reduced-selective integration [33, 34]. But these introduce other numerical problems.

With reference to works by Bathe and others [35–37], the present authors have employed the mixed interpolation of tensorial components (MITC) method, coupled to CUF, to overcome the locking phenomenon. This method has been applied to both ESL and LW variable kinematic models contained in CUF in order to analyze multilayered structures. Nine-node cylindrical shell elements have been considered. The performance of the new element has been tested by solving benchmark problems involving very thin shells as well as multilayered shells. The results show that the element has good convergence and robustness when the thicknesses become very small. In particular, the study of multilayered structures demonstrates that the zig-zag and LW models provide more accurate solutions than the simple ESL models.

## 4.2 Who First Proposed a Zig-Zag Theory?

To the best of the authors' knowledge, Lekhnitskii should be considered as the first contributor to the theory for multilayered structures. In [22], in fact, Lekhnitskii proposed a splendid method able to describe zig-zag effects (for both in-plane and through-the-thickness displacements) and interlaminar continuous transverse stresses. This is proved by Fig. 4.2, taken from Lekhnitskii's pioneering work [22], which shows an interlaminar continuous transverse shear stress field ($\tau^1$ and $\tau^2$ are shear stresses in

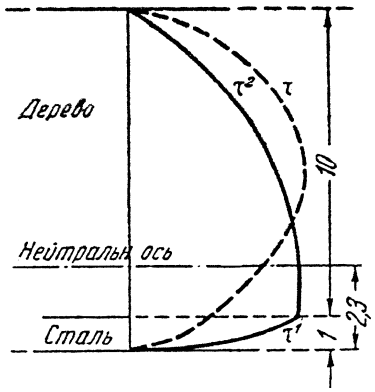


Fig. 4.2. $C_z^0$-form of a transverse shear stress in a two-layered structure.

the layers 1 and 2, respectively) with discontinuous derivatives at the layer interface (the first author thanks Prof Shifrin, who provided the original article in Russian, and D. Carrera for providing an Italian translation of the same article). In other words, the $C_z^0$–requirements of Fig. 4.1 were entirely accounted for by Lekhnitskii [22].

The authors believe it would be of relevant interest to quote the original derivations made by Lekhnitskii. It is, in fact, difficult to obtain the original article by Lekhnitskii, which has no English translation. Furthermore, the theory proposed by Lekhnitskii is very interesting and the method used could be a starting point for future developments. The following detailed derivation is therefore taken directly from Lekhnitskii's original paper, written in Russian. A few changes in notation are made. A briefer treatment can be found in the English translation of the book ([38]; Section 18 of Chapter 3, p. 74).

This section closes with a few remarks on the theory proposed by Lekhnitskii:

(1) Lekhnitskii's theory describes the zig-zag form of both longitudinal and through-the-thickness displacements, in particular:
   (a) The longitudinal displacements $u^k$ have a cubic order in the $z$–thickness direction.
   (b) The through-the-thickness displacement $w^k$ varies according to a parabolic order in $z$.

(2) Lekhnitskii's theory gives the interlaminar continuous transverse stresses $\sigma_{zz}$ and $\sigma_{xz}$.

(3) The stresses obtained by Lekhnitskii fulfill the 3D indefinite equilibrium equations (this fundamental property is intrinsic in the used stress function formulation).
(4) Stresses and displacements were obtained by employing:
   (a) Compatibility conditions for stress functions.
   (b) Strain–displacement relations.
   (c) Compatibility conditions for displacements at the interface:

$$u^{k-1} = u^k, \quad w^{k-1} = w^k, \quad k = 2, N_l. \tag{4.1}$$

   (d) Homogeneous conditions at the bottom and top surfaces for the transverse stresses:

$$\sigma_{zz}^1 = \sigma_{zz}^{N_l} = 0, \quad \sigma_{xz}^1 = \sigma_{xz}^{N_l} = 0, \quad \text{for } z = 0, h. \tag{4.2}$$

   (e) Interlaminar equilibrium for the transverse stresses:

$$\sigma_{zz}^{k-1} = \sigma_{zz}^k, \quad \sigma_{xz}^{k-1} = \sigma_{xz}^k, \quad k = 2, N_l. \tag{4.3}$$

(5) No post-processing is used to recover transverse stresses.
(6) The thickness stress $\sigma_{zz}$ are neglected. Nevertheless, the Poisson effects on the thickness displacement $w^k$ are fully retained.
(7) Full retention of Koiter's recommendation would require a different assumption for the stress functions (the authors do not know any work that does so).

Although Lekhnitskii's theory was published in the mid-1930s and reported in a short paragraph of the English edition of his book [38], it has been systematically forgotten in the recent literature. An exception is the work by Ren [39–41], which documented in the next paragraph.

### 4.3 The Lekhnitskii–Ren Theory

This is the first of the three discussed theories. It is named after the author of the original work, Lekhnitskii and the author who first extended the work to plates, Ren. Due to the original stress function formulation, the present approach could also be referred to as a "stress approach."

To the best of the authors' knowledge, Ren is the only scientist who has used Lekhnitskii's work as described in the previous section. In two papers [39, 40], Ren has, in fact, extended Lekhnitskii's theory to orthotropic and

anisotropic plates. Further applications to vibration and buckling were made in a third paper written in collaboration with Owen [41]. These three papers are the unique contributions known to the authors that have been made under the framework of Lekhnitskii's theory. As these three papers have been published in journals that are easily available worldwide, a full description of Ren's extension of Lekhnitskii's theory to plates has been, therefore, omitted. Nevertheless, it is of interest to make a few comments on Ren's work in order to make explicit the stress and displacement fields that were introduced by Ren to analyze the response of anisotropic plates.

On the basis of the form of $\tau_{xz}^k$ obtained by Lekhnitskii, it appeared reasonable to Ren, see [39], to assume the following distribution of transverse shear stresses in a laminated plate, composed of $N_l$ orthotropic layers ($x$, $y$, and $z$ are the coordinates of the reference system depicted in Fig. 4.3):

$$\begin{aligned} \sigma_{xz}^k(x,y,z) &= \xi_x(x,y)a^k(z) + \eta_x(x,y)c^k(z) \\ \sigma_{yz}^k(x,y,z) &= \xi_y(x,y)b^k(z) + \eta_y(x,y)g^k(z). \end{aligned} \tag{4.4}$$

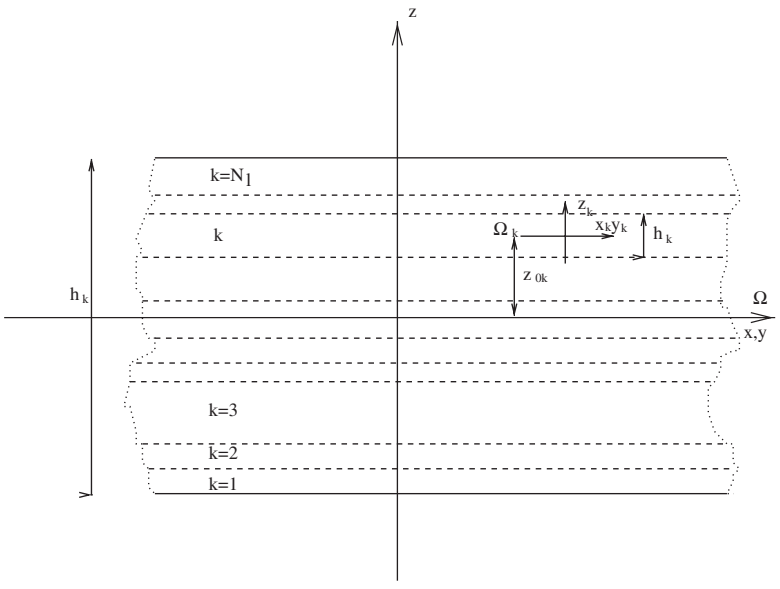


Fig. 4.3. Multilayered plate.

Four independent function of $x, y$ were introduced to describe the transverse shear stresses. The layer constants are parabolic functions of the thickness coordinate $z$. As in Lekhnitskii, the displacement fields are obtained by integrating the strain–displacement relations.

In contrast to the work by Lekhnitskii, it is underlined that the transverse strain $\epsilon_{zz}$ was discarded by Ren. This assumption contrasts with Koiter's recommendation already mentioned. The constants of integration are determined by imposing compatibility conditions for the displacements at the interface. The displacement field assumes the following form:

$$\begin{aligned} u^k(x,y,z) &= u_0(x,y) - w_{,x} + \xi_x(x,y)A^k(z) + \eta_x(x,y)C^k(z) \\ v^k(x,y,z) &= v_0(x,y) - w_{,y} + \xi_y(x,y)B^k(z) + \eta_y(x,y)G^k(z) \\ w(x,y,z) &= w_0(x,y), \end{aligned} \tag{4.5}$$

where $A^k(z)$, $B^k(z)$, $C^k(z)$, and $G^k(z)$ are obtained by integrating the corresponding $a^k(z)$, $b^k(z)$, $c^k(z)$, and $g^k(z)$. That is, Eqs. (4.5) represent a piecewise continuous displacement field in the thickness direction $z$, which is cubic in each layer. An extension to generally anisotropic layers has been provided by the same author in the article already mentioned [40].

The displacement model of Eqs. (4.5) can be used in the framework of known variational statements, such as the principle of virtual displacements (PVD) to formulate the governing equations for anisotropic plates as well as finite element models. This was done in [39–41]. No shell applications of the Lekhnitskii–Ren theory are known to the authors.

### 4.4 The Ambartsumian–Whitney–Rath–Das Theory

This is the second of the three discussed theories. Ambartsumian was the author of the original work [42–45]; Whitney [46] both extended the theory to anisotropic plates and introduced the theory to the scientific community in the West; Rath and Das [47], extended Whitney's work to shell geometries.

The Ambartsumian–Whitney–Rath–Das (AWRD) approach has the peculiarity of having the same number of unknown variables as first-order shear deformation theory, i.e. three displacements and two rotations (or shear strains). It was originated by Ambartsumian [42, 43] who restricted the formulation to orthotropic layers. Here attention will focus on the work by Whitney [46] who first applied and extended it to generally anisotropic and symmetrical and asymmetrical plates. For simplicity, only

symmetrical laminated plates are outlined. Details can be read in the above mentioned articles and books. The transverse shear stresses are assumed to be:

$$\begin{aligned}\sigma^k_{xz}(x,y,z) &= [Q^k_{55}f(z) + a^k_{55}]\phi_x(x,y) + [Q^k_{45}f(z) + a^k_{45}]\phi_y(x,y)\\ \sigma^k_{yz}(x,y,z) &= [Q^k_{45}f(z) + a^k_{55}]\phi_x(x,y) + [Q^k_{44}f(z) + a^k_{44}]\phi_y(x,y).\end{aligned} \tag{4.6}$$

The Ambartsumian case can be obtained by putting $Q^k_{45} = a^k_{45} = 0$. $f(z)$ is a function of the thickness coordinate which is assumed to be different in the symmetrical and unsymmetrical laminate cases. A parabolic form for $f(z)$ has mostly been considered (an explicit formula for unsymmetrical cases was given by Whitney). The layer constants $a^k_{44}$, $a^k_{45}$, and $a^k_{55}$ are determined by imposing the continuity conditions of transverse shear stresses at the interface while top-bottom homogeneous conditions are used to determine the form of $f(z)$. Notice that the top-bottom inhomogeneous conditions for transverse shear stresses were addressed by Ambartsumian [42, 43], along with a method to compute transverse normal stresses. These two facts have not been addressed in subsequent work.

The transverse shear strains related to the assumed transverse shear stress fields are:

$$\begin{aligned}\gamma^k_{xz}(x,y,z) &= [f(z) + S^k_{55}a^k_{55} + S^k_{45}a^k_{45}]\phi_x(x,y) + [S^k_{55}a^k_{45} + S^k_{45}a^k_{44}]\phi_y(x,y)\\ \gamma^k_{yz}(x,y,z) &= [S^k_{44}a^k_{44} + S^k_{45}a^k_{45}]\phi_x(x,y) + [f(z) + S^k_{44}a^k_{44} + S^k_{45}a^k_{55}]\phi_y(x,y),\end{aligned} \tag{4.7}$$

in which the following compliances have been introduced:

$$S^k_{55} = \frac{Q^k_{55}}{D},\quad S^k_{45} = -\frac{Q^k_{45}}{D},\quad S^k_{44} = \frac{Q^k_{44}}{D},\quad D = Q^k_{44}Q^k_{55} - (Q^k_{45})^2.$$

By assuming the transverse displacement is constant in the thickness direction, i.e. $\epsilon_{zz}$=0, on integrating the shear strains the displacement field has the following form:

$$\begin{aligned}u^k(x,y,z) &= -zw_{,x} + [J(z) + g^k_1(z)]\phi_x(x,y) + g^k_2(z)\phi_y(x,y)\\ v^k(x,y,z) &= -zw_{,y} + [J(z) + g^k_3(z)]\phi_y(x,y) + g^k_4(z)\phi_x(x,y)\\ w(x,y,x) &= w_0(x,y,z),\end{aligned} \tag{4.8}$$

where

$$\begin{aligned} J(z) &= \int f(z)dz \\ g_1^k(z) &= [S_{55}^k a_{55}^k + S_{45}^k a_{45}^k]z + d_1^k \\ g_2^k(z) &= [S_{55}^k a_{55}^k + S_{45}^k a_{45}^k]z + d_2^k \\ g_3^k(z) &= [S_{55}^k a_{55}^k + S_{45}^k a_{45}^k]z + d_3^k \\ g_4^k(z) &= [S_{55}^k a_{55}^k + S_{45}^k a_{45}^k]z + d_4^k. \end{aligned} \tag{4.9}$$

$d_1^k$, $d_2^k$, $d_3^k$ and $d_4^k$ are calculated by imposing the compatibility of the in-plane displacement at each interface. Equations (4.8) are the starting point for any analytical or computational study of multilayered plates.

An extension to doubly curved shells and a dynamic case of Whitney's work was made by Rath and Das [47].

Dozens of papers have been presented over recent decades that deal with zig-zag effects and interlaminar continuous transverse shear stresses, and which have stated that new theories were being proposed. The authors believe that these articles should be considered as simplified cases of the AWRD theory or the AWRD theory itself. Unfortunately, the original work and authors (Ambartsumian, Whitney, Rath, and Das) are not mentioned, or rarely cited, in the literature lists of this large number of articles. This historical unfairness has been corrected in [23].

### 4.5 The Reissner–Murakami–Carrera Theory

A third approach to laminated structures originated in two papers by Reissner [48, 49] in which a mixed variational equation, namely Reissner's mixed variational theorem (RMVT) was proposed. The displacement and transverse stress variables are independently assumed in RMVT. This third approach is the only one that was entirely developed in the West. Reissner [48] proposed a mixed theorem and traced the manner in which it could be developed; Murakami [50, 51], a student under Prof Reissner in San Diego, was the first to develop a plate theory on the basis of RMVT and introduced fundamental ideas on the application of RMVT in the framework of ESLM; Carrera [9, 52] presented a systematic way to use RMVT to develop plate and shell theories and introduced a weak form of Hooke's law (WFHL), which reduces mixed theories to classical models with only displacement variables.

RMVT fulfills completely and *a priori* the $C_z^0$-requirements by assuming two independent fields for displacements $\boldsymbol{u} = \{u, v, w\}$, and

transverse stresses $\boldsymbol{\sigma}_n = \{\sigma_{xz}, \sigma_{yz}, \sigma_{zz}\}$ (bold letters denote arrays). Briefly, RMVT puts 3D indefinite equilibrium equations (and related equilibrium conditions at the boundary surfaces, which for brevity are not written here) and compatibility equations for transverse strains in a variational form. The 3D equilibrium equations in the dynamic case are:

$$\sigma_{ij,j} - \rho\, \ddot{u}_i = p_i \quad i, j = 1, 2, 3, \tag{4.10}$$

where $\rho$ is the mass density and double dots denote acceleration while $(p_1, p_2, p_3) = \boldsymbol{p}$ are volume loadings. The compatibility conditions for transverse stresses can be written by evaluating transverse strains in two ways: using Hooke's law $\boldsymbol{\epsilon}_{nH} = \{\epsilon_{xz_H}, \epsilon_{yz_H}, \epsilon_{zz_H}\}$ and using a geometrical relation $\boldsymbol{\epsilon}_{nG} = \{\epsilon_{xz_G}, \epsilon_{yz_G}, \epsilon_{zz_G}\}$; the subscript $n$ denotes transverse/normal components. Hence

$$\boldsymbol{\epsilon}_{nH} - \boldsymbol{\epsilon}_{nG} = 0. \tag{4.11}$$

RMVT therefore states:

$$\begin{aligned} &\int_V (\delta \boldsymbol{\epsilon}_{pG}^T \boldsymbol{\sigma}_{pH} + \delta \boldsymbol{\epsilon}_{nG}^T \boldsymbol{\sigma}_{nM} + \delta \boldsymbol{\sigma}_{nM}^T (\boldsymbol{\epsilon}_{nG} - \boldsymbol{\epsilon}_{nH}))dV \\ &\quad = \int_V \rho \delta \boldsymbol{u}\, \ddot{\boldsymbol{u}}\, dV + \delta L_e. \end{aligned} \tag{4.12}$$

The superscript $T$ signifies an array transposition and $V$ denotes the 3D multilayered body volume while the subscript $p$ denotes in-plane components, respectively. Therefore, $\boldsymbol{\sigma}_p = \{\sigma_{xx}, \sigma_{yy}, \sigma_{xy}\}$ and $\boldsymbol{\epsilon}_p = \{\epsilon_{xx}, \epsilon_{yy}, \epsilon_{xy}\}$. The subscript $H$ underlines that stresses are computed via Hooke's law. The variation of the internal work has been split into in-plane and out-of-plane parts and involves the stress from Hooke's law and the strain from the geometrical relations (subscript $G$). $\delta L_e$ is the virtual variation of the work done by the external layer-force $\boldsymbol{p}$. Subscript $M$ underlines that transverse stresses are those of the assumed model.

The first application of RMVT was due to Murakami [50, 51], who developed a refinement of Reissner–Mindlin type theories. First a zig-zag form of the displacement field was introduced by means of two "zig-zag" functions $(D_x, D_y)$:

$$\begin{aligned} u^k(x, y, z) &= u_0(x, y) + z\phi_x(x, y) + \xi_k(-1)^k D_x(x, y) \\ v^k(x, y, z) &= v_0(x, y) + z\phi_y(x, y) + \xi_k(-1)^k D_y(x, y) \\ w(x, y, z) &= w_0(x, y). \end{aligned} \tag{4.13}$$

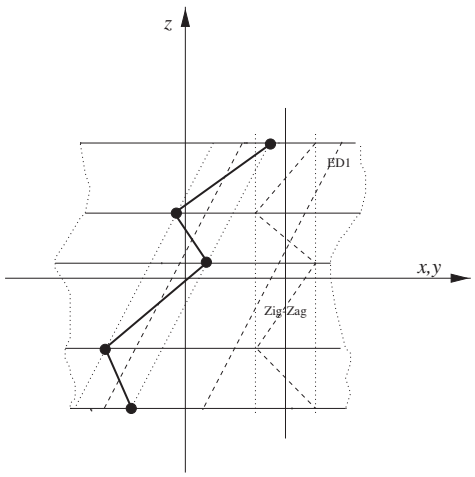


Fig. 4.4. Geometrical meaning of Murakami's zig-zag function. Linear case.

$\xi_k$=$2z_k/h_k$ is a dimensionless layer coordinate ($z_k$ is the physical coordinate of the $k$th layer whose thickness is $h_k$). The exponent $k$ changes the sign of the zig-zag term in each layer. This trick reproduces the discontinuity of the first derivative of the displacement variables in the $z$-direction. The geometrical meaning of the zig-zag function is explained in Figs. 4.4 and 4.5.

The transverse shear stresses fields were assumed to be parabolic by Murakami [50] in each layer and interlaminar continuous according to the following formula:

$$\begin{aligned}\sigma^k_{xz}(x,y,z) &= \sigma^{kt}_{xz}(x,y)F_0(z_k) + F_1(z_k)^k_x(x,y) + \sigma^{kb}_{xz}(x,y)F_2(z_k)\\ \sigma^k_{yz}(x,y,z) &= \sigma^{kt}_{yz}(x,y)F_0(z_k) + F_1(z_k)R^k_y(x,y) + \sigma^{kb}_{yz}(x,y)F_2(z_k),\end{aligned} \tag{4.14}$$

where $\sigma^{kt}_{xz}(x,y)$, $\sigma^{kt}_{yz}(x,y)$, $\sigma^{kb}_{xz}(x,y)$, and $\sigma^{kb}_{yz}(x,y)$ are the top and bottom values of the transverse shear stresses, while $R^k_x(x,y)$, and $R^k_y(x,y)$ are the layer stress resultants. The introduced layer thickness coordinate polynomials hold:

$$F_0 = -1/4 + \xi_k + 3\xi_k^2,\ F_1 = \frac{3 - 12\xi_k^2}{2h_k},\ F_2 = -1/4 - \xi_k + 3\xi_k^2.$$

The homogeneous and inhomogeneous boundary conditions at the top-bottom plate surfaces can be linked to the introduced stress field.

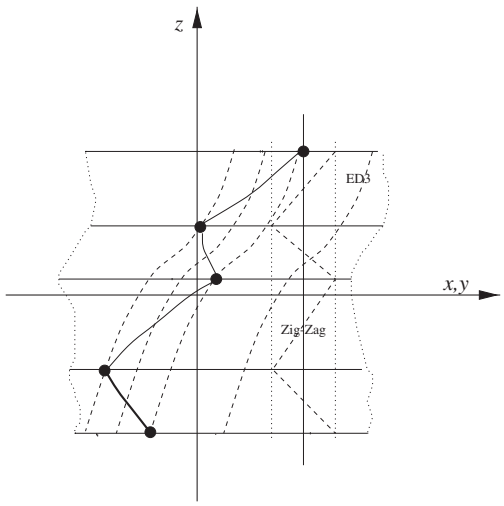


Fig. 4.5. Geometrical meaning of Murakami's zig-zag function. Higher-degree case.

Toledano and Murakami [53] introduced transverse normal strain and stress effects by using a third-order displacement field for both in-plane and out-of-plane components and a fourth-order transverse stress field for both shear and normal components. This paper is the first paper in the ESLM framework in which Koiter's recommendation is retained.

A generalization of RMVT to plate/shell theories has been provided by Carrera [28,54–60]. The displacements and transverse stress components were assumed as follows:

$$\begin{aligned} &\boldsymbol{u}^k = F_t \boldsymbol{u}_t^k + F_b \boldsymbol{u}_b^k + F_r \boldsymbol{u}_r^k = F_\tau \boldsymbol{u}_\tau^k && \tau = t, b, r \\ &&& r = 2, 3, \ldots, N \\ &\boldsymbol{\sigma}_{nM}^k = F_t \boldsymbol{\sigma}_{nt}^k + F_b \boldsymbol{\sigma}_{nb}^k + F_r \boldsymbol{\sigma}_{nr}^k = F_\tau \boldsymbol{\sigma}_{n\tau}^k && k = 1, 2, \ldots, N_l. \end{aligned} \tag{4.15}$$

The subscripts $t$ and $b$ denote values for the top and bottom surface layer, respectively. These two terms consist of the linear part of the expansion. The thickness functions $F_\tau(\xi_k)$ can now be defined at the $k$th layer level:

$$\begin{aligned} &F_t = \frac{P_0 + P_1}{2}, \quad F_b = \frac{P_0 - P_1}{2}, \quad F_r = P_r - P_{r-2}, \\ &r = 2, 3, \ldots, N \end{aligned} \tag{4.16}$$

in which $P_j = P_j(\xi_k)$ is the $j$th order Legendre polynomial defined in the $\xi_k$ domain: $-1 \leq \xi_k \leq 1$. For instance, the first five Legendre polynomials

are:

$$P_0 = 1, \quad P_1 = \xi_k, \quad P_2 = (3\xi_k^2 - 1)/2, \quad P_3 = \frac{5\xi_k^3}{2} - \frac{3\xi_k}{2},$$
$$P_4 = \frac{35\xi_k^4}{8} - \frac{15\xi_k^2}{4} + \frac{3}{8}.$$

The chosen functions have the following properties:

$$\xi_k = \begin{cases} 1 \text{ when } F_t = 1;\ F_b = 0;\ F_r = 0 \\ -1 \text{ when } F_t = 0;\ F_b = 1;\ F_r = 0. \end{cases} \tag{4.17}$$

The top and bottom values have been used as unknown variables. Such a choice makes the model particularly suitable, in view of the fulfillment of the $C_z^0$-requirements. The interlaminar transverse shear and normal stress continuity can therefore be linked by simply writing:

$$\boldsymbol{\sigma}_{nt}^k = \boldsymbol{\sigma}_{nb}^{k+1}, \quad k = 1, N_l - 1. \tag{4.18}$$

In those cases in which the top/bottom plate/shell stress values are prescribed (zero or imposed values), the following additional equilibrium conditions must be accounted for:

$$\boldsymbol{\sigma}_{nb}^1 = \bar{\boldsymbol{\sigma}}_{nb}, \quad \boldsymbol{\sigma}_{nt}^{N_l} = \bar{\boldsymbol{\sigma}}_{nt}, \tag{4.19}$$

where the over-bar denotes the imposed values for the plate boundary surfaces.

Examples of the application of RMVT to laminated plates in the equivalent single-layer model were presented in the already mentioned articles [50, 51, 53]. The results obtained for the cylindrical bending of cross-ply symmetrically laminated plates showed an improvement in describing the in-plane response with respect to the first-order shear deformation theory [51]. Applications to unsymmetrically laminated plates were presented in [53]. Shell applications based on [51] were developed by Bhaskar and Varadan [61] and Jing and Tzeng [62]. Bhaskar and Varadan [61] underlined the severe limitation of the transverse shear stress *a priori* evaluated by the assumed model. Finite element applications of this model have been developed. The linear analysis of thick plates was discussed by Rao and Meyer-Piening [63]. Linear and geometrically non-linear static and dynamic analyses were considered by Carrera [54, 64] and co-authors [65]. Partial implementations to shell elements were proposed by Bhaskar and Varadan [66]. A full shell implementation has recently been given by Brank and Carrera [67].

The limitations of the equivalent single-layer analysis were known to Toledano and Murakami [53] who applied RMVT in a multilayered model. A linear in-plane displacement expansion was expressed in terms of the interface values in each layer while the transverse shear stresses were assumed parabolic. It was shown that the accuracy of the resulting theories was independent of layout. Transverse normal stress and related effects were discarded and the analysis showed severe limitations when analyzing thick plates. A more comprehensive evaluation of layer-wise theories for linear and parabolic expansions was made by the first author in [55] where applications to the static analysis of plates were presented. Subsequent work extended the analysis to dynamic cases [28, 56, 59, 60] and shell geometry [52, 57, 58]. A more exhaustive overview work of based on Reissner's theorem has been provided in [19].

### 4.6 Remarks on the Theories

In the authors' opinion the work by Lekhnitskii is the most relevant contribution to multilayered structure modeling:

- L1. This is the *first* work to account for the $C_z^0$-requirements.
- L2. Even though Lekhnitskii restricted his analysis to a cantilevered multilayered beam, he quoted explicit formulas for transverse stresses and displacement fields (Eqs. (4.4) and (4.5)), which are valid at all points of the considered beam. This could be extremely useful in assessing new analytical and numerical models.
- L3. The work by Lekhnitskii shows how multilayered structures problems can be handled. For instance, it is clear in [22] that the inclusion of a transverse normal stress would require a different choice of stress functions.
- L4. The stress function formulation leads to in-plane and transverse stress fields which fulfill "by definition" the 3D equilibrium equations. Stresses were calculated by Lekhnitskii by solving a boundary-value problem for the compatibility equations written in terms of a stress function. In particular, the evaluation of transverse stresses does not require any post-processing procedure such as Hooke's law or integration of 3D equilibrium equations.
- L5. Although transverse normal stresses are neglected, the transverse displacement varies in the beam thickness according to a piecewise-parabolic distribution. A direct attempt to include the transverse

normal stress effect would require an appropriate choice for the stress function.

Concerning Lekhnitskii–Ren plate theory observe that:

- LR1. The transverse shear stresses are continuous at the interfaces and parabolic in each layer. Furthermore, homogeneous conditions are fulfilled at the top-bottom plate surfaces.
- LR2. Four independent functions defined on $\Omega$ are used to express transverse shear stresses. Layer constants, which are parabolic in each layer, are used to describe the transverse shear stresses.
- LR3. Expressions for the layer constants were given by Ren. In other words their calculation does not require any imposition of transverse shear stresses.
- LR4. The in-plane displacements are continuous at each interface and are cubic in each layer.
- LR5. Seven independent variables defined on $\Omega$ were used to describe the displacement and stress fields in the laminated plates. Four are used for the transverse shear stresses and three for the displacements corresponding to the chosen reference surface $\Omega$.
- LR6. According to Lekhnitskii, Ren neglects the transverse normal stress $\sigma_{zz}$. In contrast to Lekhnitskii, the transverse normal strain $\epsilon_{zz}$ is discarded by Ren.
- LR7. The transverse shear stresses are calculated by Ren directly using Eqs. (4.4). Hooke's Law is not used and integration of the 3D equilibrium equations is not required.

Regarding the Ambartsumian–Whitney–Rath–Das theory notice that:

- AWRD1. As LR1.
- AWRD2. Two independent functions defined on $\Omega$ are used to express transverse shear stresses (Eqs. (4.6)).
- AWRD3. Layer constants, parabolic in each layer, must be computed by imposing transverse shear stress continuity at each interface while the form of the $f(z)$ function is found by imposing top-bottom layer homogeneous conditions.
- AWRD4. As LR4.
- AWRD5. Five independent variables defined on $\Omega$ are used to describe the displacement and stress fields in a laminated plate/shell, which is two less than LR.
- AWRD6. As LR6.

- AWRD7. The literature shows that much better evaluations for transverse shear stresses are obtained via integration of the 3D equilibrium equations, with respect to Eqs. (4.6).
- AWRD8. The extension to a shell requires a reformulation of the displacement models and related layer constants.

For the Reissner–Murakami–Carrera theory observe that:

- RMC1. As LR1. In this case, homogeneous as well as inhomogeneous conditions for transverse stresses can be included.
- RMC2. At least $2N_l + 1$ independent variables must be used for each transverse stress component. However, these variables can be expressed in terms of the displacement variables using a weak form of Hooke's law.
- RMC3. The in-plane displacements are continuous at each interface and can be chosen linear or of higher order in each layer.
- RMC4. The number of independent variables can be chosen arbitrarily according to RMC3.
- RMC5. Interlaminar continuous transverse normal stresses/strains can be easily described by the RMC theory. These effects were, in fact, included in the early development of the RMC theory, fulfilling the fundamental Koiter's recommendation.
- RMC6. As for the AWRD theory much better evaluations for transverse stresses are obtained via integration of the 3D equilibrium equations, with respect to assumed forms, e.g. Eqs. (4.14).
- RMC7. The extension to a shell does not require any changes in either displacement or stress fields.

### 4.7 A Brief Discussion on Layer-Wise Theories

The previous discussion has been restricted to ESLM. In this class of theories the number of unknown variables doesn't depend on the number of layers (it is intended that for the RMC theory this restriction is only for displacement variables). The use of independent variables in each layer, as in the layer-wise description, increases computational costs. On the other hand, such a choice permits one to include "naturally" the zig-zag form of displacements in the thickness direction and in general can significantly improve for the response of very thick structures. In this respect, the authors' experience suggests that the layer-wise description is mandatory for thick plate/shell analyses and in any other problems in

which the response is essentially a layer response. In particular, in [60] the first author showed that the use of a sufficiently high order for the displacement fields in the layers could lead to a description with acceptable accuracy of the transverse stresses directly computed by Hooke's law. Many layer-wise theories have been proposed. So called global/local approaches have also been proposed, see Reddy [21]. Excellent overviews can be found in the review articles and books mentioned in the Introduction.

To the best of the authors' knowledge, there is no layer-wise theory based on the LR approach. Works with a layer-wise description in the framework of the AWRD theories have recently been discussed by Cho and Averill [68]. Studies on the use of the RMC theory have been made for plates by Toledano and Murakami [53] and extended to higher-order cases (including normal stress effects), dynamics, and shells in the Carrera's articles [55, 60].

### 4.8 CUF Shell Finite Elements

The efficient load-carrying capabilities of shell structures make them very useful in a variety of engineering applications. The continuous development of new structural materials leads to ever more complex structural designs that require careful analysis. Although analytical techniques are very important, the use of numerical methods to solve mathematical shell models of complex structures has become an essential ingredient in the design process. The finite element method (FEM) has been the fundamental numerical procedure in the analysis of shells.

In this section, a new shell finite element approach based on variable kinematic models within Carrera's unified formulation [27, 28] is presented. Elements with nine nodes and cylindrical geometry are considered. Referring to Bathe and others [35–37], the MITC method is used to overcome the locking phenomenon. The governing equations are derived in the framework of the CUF in order to apply FEM. Some numerical results are provided to show the efficiency of the new element.

#### 4.8.1 *Geometry of cylindrical shells*

Let us consider a cylindrical shell. In a system of Cartesian coordinates $(O, x, y, z)$, the region occupied by the mid-surface of the shell is:

$$S = \{(x, y, z) \in R^3 : \ -L/2 < x < L/2, \ y^2 + z^2 = R^2\} \tag{4.20}$$

where $L$ and $R$ are the length and the radius of the shell, respectively. Let us consider a curvilinear coordinate system $(\alpha, \beta, z)$ placed at the center of the upper part of the mid-surface. The 3D medium corresponding to the shell is defined by the 3D chart given by:

$$\boldsymbol{\Phi}(\alpha, \beta, z) = \boldsymbol{\phi}(\alpha, \beta) + z\boldsymbol{a}_3(\alpha, \beta), \tag{4.21}$$

where $\boldsymbol{a}_3$ is the unit vector normal to the tangent plane. Then, the mid-surface $S$ of the cylindrical shell is described by the following 2D chart:

$$\begin{cases} \phi_1(\alpha, \beta) = \alpha \\ \phi_2(\alpha, \beta) = R\sin(\beta/R) \\ \phi_3(\alpha, \beta) = R\cos(\beta/R). \end{cases} \tag{4.22}$$

With this choice, the region $\Omega \subset R^2$ corresponding to the mid-surface $S$ is the rectangle:

$$\Omega = \{(\alpha, \beta) : \ -L/2 < \alpha < L/2, \ -R\pi < \beta < R\pi\}. \tag{4.23}$$

Using these geometrical assumptions, the strain–displacement relations can be obtained by considering the linear part of the *3D Green–Lagrange strain tensor*. Remembering that in the unified formulation the unknowns are the components of the displacement $u_\tau(\alpha, \beta)$, $v_\tau(\alpha, \beta)$, and $w_\tau(\alpha, \beta)$, for $\tau = 0, 1, \ldots, N$, the *geometrical relations* for the $k$th layer of a multilayer cylindrical shell can be written as follow:

$$\begin{aligned} \varepsilon^k_{\alpha\alpha} &= F_\tau u^k_{\tau,\alpha} \\ \varepsilon^k_{\beta\beta} &= F_\tau \left[ \left(1 + \frac{z_k}{R_k}\right) \frac{w^k_\tau}{R_k} + \left(1 + \frac{z_k}{R_k}\right) v^k_{\tau,\beta} \right] \\ \varepsilon^k_{\alpha\beta} &= F_\tau \left[ u^k_{\tau,\beta} + \left(1 + \frac{z_k}{R_k}\right) v^k_{\tau,\alpha} \right] \\ \varepsilon^k_{\alpha z} &= w^k_{\tau,\alpha} F_\tau + u^k_\tau F_{\tau,z} \\ \varepsilon^k_{\beta z} &= F_\tau \left[ w^k_{\tau,\beta} - \frac{v^k_\tau}{R_k} \right] + F_{\tau,z} \left[ \left(1 + \frac{z_k}{R_k}\right) v^k_\tau \right] \\ \varepsilon^k_{zz} &= w^k_\tau F_{\tau,z}, \end{aligned} \tag{4.24}$$

where $R_k$ is the radius of the mid-surface of the layer $k$. The thickness functions $F_\tau$ are Taylor functions $(1, z, z^2, \ldots)$ if the approach used is ESL or combinations of Legendre polynomials if the approach is LW (see Eqs. (4.16)). For more details of the geometrical description and the

procedure to obtain the strain–displacement relations, the reader can refer to [69].

The previous geometrical relations can be expressed in matrix form as:

$$\begin{aligned} \boldsymbol{\varepsilon}_p^k &= (\boldsymbol{D}_p^k + \boldsymbol{A}_p^k)\boldsymbol{u}^k \\ \boldsymbol{\varepsilon}_n^k &= (\boldsymbol{D}_{n\Omega}^k + \boldsymbol{D}_{nz}^k - \boldsymbol{A}_n^k)\boldsymbol{u}^k, \end{aligned} \tag{4.25}$$

where subscripts $(p)$ and $(n)$ indicate in-plane and normal components, respectively, and the differential operators are defined as follows:

$$\boldsymbol{D}_p^k = \begin{bmatrix} \partial_\alpha & 0 & 0 \\ 0 & H_k\partial_\beta & 0 \\ \partial_\beta & H_k\partial_\alpha & 0 \end{bmatrix}, \quad \boldsymbol{D}_{n\Omega}^k = \begin{bmatrix} 0 & 0 & \partial_\alpha \\ 0 & 0 & \partial_\beta \\ 0 & 0 & 0 \end{bmatrix},$$

$$\boldsymbol{D}_{nz}^k = \partial_z \cdot \boldsymbol{A}_{nz}^k = \partial_z \begin{bmatrix} 1 & 0 & 0 \\ 0 & H_k & 0 \\ 0 & 0 & 1 \end{bmatrix}, \tag{4.26}$$

$$\boldsymbol{A}_p^k = \begin{bmatrix} 0 & 0 & 0 \\ 0 & 0 & \frac{1}{R_k}H_k \\ 0 & 0 & 0 \end{bmatrix}, \quad \boldsymbol{A}_n^k = \begin{bmatrix} 0 & 0 & 0 \\ 0 & \frac{1}{R_k} & 0 \\ 0 & 0 & 0 \end{bmatrix}, \tag{4.27}$$

where $H_k = (1 + z_k/R_k)$.

### 4.8.2 *MITC method*

Considering the components of the strain tensor in the local coordinate system $(\xi, \eta, z)$, the MITC shell elements are formulated using – instead of the strain components directly computed from the displacements – an interpolation of these strain components within each element using a specific interpolation strategy for each component. The corresponding interpolation points — called the *tying points*— are shown in Fig. 4.6 for a nine-node shell element (MITC9 shell element). For more details see [69].

The interpolating functions are arranged in the following arrays:

$$\begin{aligned} N_{m1} &= [N_{A1}, N_{B1}, N_{C1}, N_{D1}, N_{E1}, N_{F1}] \\ N_{m2} &= [N_{A2}, N_{B2}, N_{C2}, N_{D2}, N_{E2}, N_{F2}] \\ N_{m3} &= [N_P, N_Q, N_R, N_S]. \end{aligned} \tag{4.28}$$

For convenience, we will indicate with the subscripts $m1$, $m2$, and $m3$ the quantities calculated for the points $(A1, B1, C1, D1, E1, F1)$, $(A2, B2, C2, D2, E2, F2)$, and $(P, Q, R, S)$, respectively.

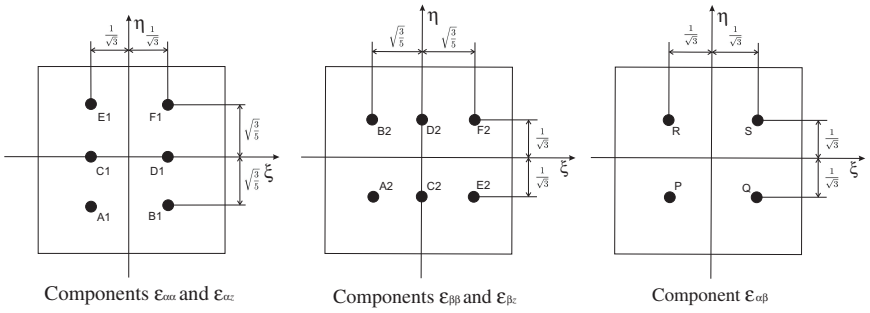


Fig. 4.6. Tying points for MITC9 shell finite element.

According to the MITC method, the strain components are interpolated on the tying points as follows:

$$\boldsymbol{\varepsilon}_p^k = \begin{bmatrix} \varepsilon_{11}^k \\ \varepsilon_{22}^k \\ \varepsilon_{12}^k \end{bmatrix} = \begin{bmatrix} N_{m1} & 0 & 0 \\ 0 & N_{m2} & 0 \\ 0 & 0 & N_{m3} \end{bmatrix} \begin{bmatrix} \varepsilon_{11_{m1}}^k \\ \varepsilon_{22_{m2}}^k \\ \varepsilon_{12_{m3}}^k \end{bmatrix} = [\boldsymbol{N1}] \begin{bmatrix} \varepsilon_{11_{m1}}^k \\ \varepsilon_{22_{m2}}^k \\ \varepsilon_{12_{m3}}^k \end{bmatrix}$$
$$\boldsymbol{\varepsilon}_n^k = \begin{bmatrix} \varepsilon_{13}^k \\ \varepsilon_{23}^k \\ \varepsilon_{33}^k \end{bmatrix} = \begin{bmatrix} N_{m1} & 0 & 0 \\ 0 & N_{m2} & 0 \\ 0 & 0 & 1 \end{bmatrix} \begin{bmatrix} \varepsilon_{13_{m1}}^k \\ \varepsilon_{23_{m2}}^k \\ \varepsilon_{33}^k \end{bmatrix} = [\boldsymbol{N2}] \begin{bmatrix} \varepsilon_{13_{m1}}^k \\ \varepsilon_{23_{m2}}^k \\ \varepsilon_{33}^k \end{bmatrix}, \tag{4.29}$$

which defines the matrixes $\boldsymbol{N1}$ and $\boldsymbol{N2}$.

Applying the finite element method, the unknown displacements are interpolated on the nodes of the element by means of the Lagrangian shape functions $N_i$ (for $i = 1, \ldots, 9$):

$$\boldsymbol{u}^k = F_\tau N_i \boldsymbol{q}_{\tau_i}^k, \tag{4.30}$$

where $\boldsymbol{q}_{\tau_i}^k$ are the nodal displacements and the unified formulation is applied. Substituting in Eqs. (4.25) the geometrical relations become:

$$\begin{aligned} \boldsymbol{\varepsilon}_p^k =& F_\tau (\boldsymbol{D}_p^k + \boldsymbol{A}_p^k)(N_i \boldsymbol{I}) \boldsymbol{q}_{\tau_i}^k \\ \boldsymbol{\varepsilon}_n^k =& F_\tau (\boldsymbol{D}_{n\Omega}^k - \boldsymbol{A}_n^k)(N_i \boldsymbol{I}) \boldsymbol{q}_{\tau_i}^k + F_{\tau,z} \boldsymbol{A}_{nz}^k (N_i \boldsymbol{I}) \boldsymbol{q}_{\tau_i}^k, \end{aligned} \tag{4.31}$$

where $\boldsymbol{I}$ is a $3 \times 3$ identity matrix.

If the MITC technique is applied, the geometrical relations are rewritten as follows:

$$\begin{aligned} \boldsymbol{\varepsilon}_{p_{im}}^{k\tau} &= F_\tau[\boldsymbol{C}_{3_{im}}^k]\boldsymbol{q}_{\tau_i}^k \\ \boldsymbol{\varepsilon}_{n_{im}}^{k\tau} &= F_\tau[\boldsymbol{C}_{1_{im}}^k]\boldsymbol{q}_{\tau_i}^k + F_{\tau,z}[\boldsymbol{C}_{2_{im}}^k]\boldsymbol{q}_{\tau_i}^k, \end{aligned} \tag{4.32}$$

where the introduced matrixes are:

$$\begin{aligned} [\boldsymbol{C}_{1_{im}}^k] &= [\boldsymbol{N2}] \begin{bmatrix} [(\boldsymbol{D}_{n\Omega}^k - \boldsymbol{A}_n^k)(N_i\boldsymbol{I})]_{m1}(1,:) \\ [(\boldsymbol{D}_{n\Omega}^k - \boldsymbol{A}_n^k)(N_i\boldsymbol{I})]_{m2}(2,:) \\ [(\boldsymbol{D}_{n\Omega}^k - \boldsymbol{A}_n^k)(N_i\boldsymbol{I})](3,:) \end{bmatrix} \\ [\boldsymbol{C}_{2_{im}}^k] &= [\boldsymbol{N2}] \begin{bmatrix} [\boldsymbol{A}_{nz}^k(N_i\boldsymbol{I})]_{m1}(1,:) \\ [\boldsymbol{A}_{nz}^k(N_i\boldsymbol{I})]_{m2}(2,:) \\ [\boldsymbol{A}_{nz}^k(N_i\boldsymbol{I})](3,:) \end{bmatrix} \\ [\boldsymbol{C}_{3_{im}}^k] &= [\boldsymbol{N1}] \begin{bmatrix} [(\boldsymbol{D}_p^k + \boldsymbol{A}_p^k)(N_i\boldsymbol{I})]_{m1}(1,:) \\ [(\boldsymbol{D}_p^k + \boldsymbol{A}_p^k)(N_i\boldsymbol{I})]_{m2}(2,:) \\ [(\boldsymbol{D}_p^k + \boldsymbol{A}_p^k)(N_i\boldsymbol{I})]_{m3}(3,:) \end{bmatrix}. \end{aligned} \tag{4.33}$$

(1,:), (2,:), and (3,:) respectively indicate that the first, second, or third line of the relevant matrix is considered.

### 4.8.3 *Governing equations*

This section presents the derivation of the governing equations based on the *principle of virtual displacements* (PVD) for a multilayered shell subjected to mechanical loads. CUF can be used to obtain the so-called *fundamental nuclei*, which are simple matrices representing the basic elements from which the stiffness matrix of the whole structure can be computed.

The PVD for a multilayered shell with $N_l$ layers is:

$$\sum_{k=1}^{N_l} \int_{\Omega_k} \int_{A_k} \left\{ \delta {\boldsymbol{\epsilon}_{pG}^k}^T \boldsymbol{\sigma}_{pC}^k + \delta {\boldsymbol{\epsilon}_{nG}^k}^T \boldsymbol{\sigma}_{nC}^k \right\} d\Omega_k dz_k = \sum_{k=1}^{N_l} \delta L_e^k, \tag{4.34}$$

where $\Omega_k$ and $A_k$ are the integration domains in the plane ($\alpha$,$\beta$) and the $z$-direction, respectively, and $T$ indicates the transpose of a vector. The first member of the equation represents the variation of internal work $\delta L_{int}^k$ and $\delta L_e^k$ is the external work. $G$ means geometrical relations and $C$ constitutive relations. The first step in deriving the fundamental nuclei is the substitution of the *constitutive equations* ($C$) in the variational

statement of PVD, which are:

$$\begin{aligned} \boldsymbol{\sigma}^k_{pC} = \boldsymbol{\sigma}^{ks}_{p_{jn}} &= \boldsymbol{C}^k_{pp}\, \boldsymbol{\varepsilon}^{ks}_{p_{jn}} + \boldsymbol{C}^k_{pn}\, \boldsymbol{\varepsilon}^{ks}_{n_{jn}} \\ \boldsymbol{\sigma}^k_{nC} = \boldsymbol{\sigma}^{ks}_{n_{jn}} &= \boldsymbol{C}^k_{np}\, \boldsymbol{\varepsilon}^{ks}_{p_{jn}} + \boldsymbol{C}^k_{nn}\, \boldsymbol{\varepsilon}^{ks}_{n_{jn}} \end{aligned} \tag{4.35}$$

with

$$\begin{aligned} \boldsymbol{C}^k_{pp} &= \begin{bmatrix} C^k_{11} & C^k_{12} & C^k_{16} \\ C^k_{12} & C^k_{22} & C^k_{26} \\ C^k_{16} & C^k_{26} & C^k_{66} \end{bmatrix} \quad \boldsymbol{C}^k_{pn} = \begin{bmatrix} 0 & 0 & C^k_{13} \\ 0 & 0 & C^k_{23} \\ 0 & 0 & C^k_{36} \end{bmatrix} \\ \boldsymbol{C}^k_{np} &= \begin{bmatrix} 0 & 0 & 0 \\ 0 & 0 & 0 \\ C^k_{13} & C^k_{23} & C^k_{36} \end{bmatrix} \quad \boldsymbol{C}^k_{nn} = \begin{bmatrix} C^k_{55} & C^k_{45} & 0 \\ C^k_{45} & C^k_{44} & 0 \\ 0 & 0 & C^k_{33} \end{bmatrix}, \end{aligned} \tag{4.36}$$

and $C$ are the material coefficients.

Then, one substitutes the geometrical relations (4.32) and the constitutive equations (4.35) into the variational statement (4.34) to obtain the governing equation system:

$$\delta \boldsymbol{u}^{k\,T}_{\tau i} : \quad \boldsymbol{K}^{k\tau sij}_{uu} \boldsymbol{u}^k_{sj} = \boldsymbol{P}^k_{u\tau i}, \tag{4.37}$$

where $\boldsymbol{K}^{k\tau sij}_{uu}$ is the fundamental nucleus of the stiffness array, which is expanded according to the indexes $\tau$,$s$ and $i$,$j$ in order to obtain the matrix for the whole shell. $\boldsymbol{P}^k_{u\tau}$ is the fundamental nucleus of the external mechanical load. The explicit form of the stiffness fundamental nucleus is the following:

$$\begin{aligned} K^{k\tau sij}_{11} = {} & C^k_{55} N_{i_{m1}} \lhd N_{m1} N_{n1} \rhd_{\Omega_k} N_{j_{n1}} \lhd F_{\tau_{,z}} F_{s_{,z}} \rhd_{A_k} \\ & + C^k_{11} N_{i,\alpha_{m1}} \lhd N_{m1} N_{n1} \rhd_{\Omega_k} N_{j,\alpha_{n1}} \lhd F_\tau F_s \rhd_{A_k} \\ & + C^k_{16} N_{i,\beta_{m3}} \lhd N_{m3} N_{n1} \rhd_{\Omega_k} N_{j,\alpha_{n1}} \lhd F_\tau F_s \rhd_{A_k} \\ & + C^k_{16} N_{i,\alpha_{m1}} \lhd N_{m1} N_{n3} \rhd_{\Omega_k} N_{j,\beta_{n3}} \lhd F_\tau F_s \rhd_{A_k} \\ & + C^k_{66} N_{i,\beta_{m3}} \lhd N_{m3} N_{n3} \rhd_{\Omega_k} N_{j,\beta_{n3}} \lhd F_\tau F_s \rhd_{A_k} \\ K^{k\tau sij}_{12} = {} & -C^k_{45} \frac{1}{R_k} N_{i_{m1}} \lhd N_{m1} N_{n2} \rhd_{\Omega_k} N_{j_{n2}} \lhd F_{\tau_{,z}} F_s \rhd_{A_k} \\ & + C^k_{45} N_{i_{m1}} \lhd N_{m1} N_{n2} \rhd_{\Omega_k} N_{j_{n2}} \lhd H_k F_{\tau_{,z}} F_{s_{,z}} \rhd_{A_k} \end{aligned}$$

$$
\begin{aligned}
&+C^k_{12} N_{i,\alpha_{m1}} \lhd N_{m1} N_{n2} \rhd_{\Omega_k} N_{j,\beta_{n2}} \lhd H_k F_\tau F_s \rhd_{A_k} \\
&+C^k_{16} N_{i,\alpha_{m1}} \lhd N_{m1} N_{n3} \rhd_{\Omega_k} N_{j,\alpha_{n3}} \lhd H_k F_\tau F_s \rhd_{A_k} \\
&+C^k_{26} N_{i,\beta_{m3}} \lhd N_{m3} N_{n2} \rhd_{\Omega_k} N_{j,\beta_{n2}} \lhd H_k F_\tau F_s \rhd_{A_k} \\
&+C^k_{66} N_{i,\beta_{m3}} \lhd N_{m3} N_{n3} \rhd_{\Omega_k} N_{j,\alpha_{n3}} \lhd H_k F_\tau F_s \rhd_{A_k}
\end{aligned} \tag{4.38}
$$

$$
\begin{aligned}
K^{k\tau sij}_{13} = {} & C^k_{13} N_{i,\alpha_{m1}} \lhd N_{m1} N_j \rhd_{\Omega_k} \lhd F_\tau F_{s,z} \rhd_{A_k} \\
&+C^k_{36} N_{i,\beta_{m3}} \lhd N_{m3} N_j \rhd_{\Omega_k} \lhd F_\tau F_{s,z} \rhd_{A_k} \\
&+C^k_{12} \frac{1}{R_k} N_{i,\alpha_{m1}} \lhd N_{m1} N_{n2} \rhd_{\Omega_k} N_{j_{n2}} \lhd H_k F_\tau F_s \rhd_{A_k} \\
&+C^k_{26} \frac{1}{R_k} N_{i,\beta_{m3}} \lhd N_{m3} N_{n2} \rhd_{\Omega_k} N_{j_{n2}} \lhd H_k F_\tau F_s \rhd_{A_k} \\
&+C^k_{55} N_{i_{m1}} \lhd N_{m1} N_{n1} \rhd_{\Omega_k} N_{j,\alpha_{n1}} \lhd F_{\tau,z} F_s \rhd_{A_k} \\
&+C^k_{45} N_{i_{m1}} \lhd N_{m1} N_{n2} \rhd_{\Omega_k} N_{j,\beta_{n2}} \lhd F_{\tau,z} F_s \rhd_{A_k}
\end{aligned}
$$

$$
\begin{aligned}
K^{k\tau sij}_{21} = {} & -C^k_{45} \frac{1}{R_k} N_{i_{m2}} \lhd N_{m2} N_{n1} \rhd_{\Omega_k} N_{j_{n1}} \lhd F_\tau F_{s,z} \rhd_{A_k} \\
&+C^k_{45} N_{i_{m2}} \lhd N_{m2} N_{n1} \rhd_{\Omega_k} N_{j_{n1}} \lhd H_k F_{\tau,z} F_{s,z} \rhd_{A_k} \\
&+C^k_{12} N_{i,\beta_{m2}} \lhd N_{m2} N_{n1} \rhd_{\Omega_k} N_{j,\alpha_{n1}} \lhd H_k F_\tau F_s \rhd_{A_k} \\
&+C^k_{16} N_{i,\alpha_{m3}} \lhd N_{m3} N_{n1} \rhd_{\Omega_k} N_{j,\alpha_{n1}} \lhd H_k F_\tau F_s \rhd_{A_k} \\
&+C^k_{26} N_{i,\beta_{m2}} \lhd N_{m2} N_{n3} \rhd_{\Omega_k} N_{j,\beta_{n3}} \lhd H_k F_\tau F_s \rhd_{A_k} \\
&+C^k_{66} N_{i,\alpha_{m3}} \lhd N_{m3} N_{n3} \rhd_{\Omega_k} N_{j,\beta_{n3}} \lhd H_k F_\tau F_s \rhd_{A_k}
\end{aligned}
$$

$$
\begin{aligned}
K^{k\tau sij}_{22} = {} & C^k_{22} N_{i,\beta_{m2}} \lhd N_{m2} N_{n2} \rhd_{\Omega_k} N_{j,\beta_{n2}} \lhd H^2_k F_\tau F_s \rhd_{A_k} \\
&+C^k_{26} N_{i,\beta_{m2}} \lhd N_{m2} N_{n3} \rhd_{\Omega_k} N_{j,\alpha_{n3}} \lhd H^2_k F_\tau F_s \rhd_{A_k} \\
&+C^k_{26} N_{i,\alpha_{m3}} \lhd N_{m3} N_{n2} \rhd_{\Omega_k} N_{j,\beta_{n2}} \lhd H^2_k F_\tau F_s \rhd_{A_k} \\
&+C^k_{66} N_{i,\alpha_{m3}} \lhd N_{m3} N_{n3} \rhd_{\Omega_k} N_{j,\alpha_{n3}} \lhd H^2_k F_\tau F_s \rhd_{A_k} \\
&+C^k_{44} \frac{1}{R^2_k} N_{i_{m2}} \lhd N_{m2} N_{n2} \rhd_{\Omega_k} N_{j_{n2}} \lhd F_\tau F_s \rhd_{A_k} \\
&-C^k_{44} \frac{1}{R_k} N_{i_{m2}} \lhd N_{m2} N_{n2} \rhd_{\Omega_k} N_{j_{n2}} \lhd H_k F_\tau F_{s,z} \rhd_{A_k} \\
&-C^k_{44} \frac{1}{R_k} N_{i_{m2}} \lhd N_{m2} N_{n2} \rhd_{\Omega_k} N_{j_{n2}} \lhd H_k F_{\tau,z} F_s \rhd_{A_k} \\
&+C^k_{44} N_{i_{m2}} \lhd N_{m2} N_{n2} \rhd_{\Omega_k} N_{j_{n2}} \lhd H^2_k F_{\tau,z} F_{s,z} \rhd_{A_k}
\end{aligned} \tag{4.39}
$$

$$
\begin{aligned}
K_{23}^{k\tau sij} = {} & C_{22}^{k}\frac{1}{R_k}N_{i,\beta_{m2}} \lhd N_{m2}N_{n2} \rhd_{\Omega_k} N_{j_{n2}} \lhd H_k^2 F_\tau F_s \rhd_{A_k} \\
& + C_{23}^{k} N_{i,\beta_{m2}} \lhd N_{m2}N_j \rhd_{\Omega_k} \lhd H_k F_\tau F_{s_{,z}} \rhd_{A_k} \\
& + C_{26}^{k}\frac{1}{R_k}N_{i,\alpha_{m3}} \lhd N_{m3}N_{n2} \rhd_{\Omega_k} N_{j_{n2}} \lhd H_k^2 F_\tau F_s \rhd_{A_k} \\
& + C_{36}^{k} N_{i,\alpha_{m3}} \lhd N_{m3}N_j \rhd_{\Omega_k} \lhd H_k F_\tau F_{s_{,z}} \rhd_{A_k} \\
& - C_{45}^{k}\frac{1}{R_k}N_{i_{m2}} \lhd N_{m2}N_{n1} \rhd_{\Omega_k} N_{j,\alpha_{n1}} \lhd F_\tau F_s \rhd_{A_k} \\
& - C_{44}^{k}\frac{1}{R_k}N_{i_{m2}} \lhd N_{m2}N_{n2} \rhd_{\Omega_k} N_{j,\beta_{n2}} \lhd F_\tau F_s \rhd_{A_k} \\
& + C_{45}^{k} N_{i_{m2}} \lhd N_{m2}N_{n1} \rhd_{\Omega_k} N_{j,\alpha_{n1}} \lhd H_k F_{\tau_{,z}} F_s \rhd_{A_k} \\
& + C_{44}^{k} N_{i_{m2}} \lhd N_{m2}N_{n2} \rhd_{\Omega_k} N_{j,\beta_{n2}} \lhd H_k F_{\tau_{,z}} F_s \rhd_{A_k} \\
K_{31}^{k\tau sij} = {} & C_{55}^{k} N_{i,\alpha_{m1}} \lhd N_{m1}N_{n1} \rhd_{\Omega_k} N_{j_{n1}} \lhd F_\tau F_{s_{,z}} \rhd_{A_k} \\
& + C_{45}^{k} N_{i,\beta_{m2}} \lhd N_{m2}N_{n1} \rhd_{\Omega_k} N_{j_{n1}} \lhd F_\tau F_{s_{,z}} \rhd_{A_k} \\
& + C_{12}^{k}\frac{1}{R_k}N_{i_{m2}} \lhd N_{m2}N_{n1} \rhd_{\Omega_k} N_{j,\alpha_{n1}} \lhd H_k F_\tau F_s \rhd_{A_k} \\
& + C_{13}^{k} \lhd N_i N_{n1} \rhd_{\Omega_k} N_{j,\alpha_{n1}} \lhd F_{\tau_{,z}} F_s \rhd_{A_k} \\
& + C_{26}^{k}\frac{1}{R_k}N_{i_{m2}} \lhd N_{m2}N_{n3} \rhd_{\Omega_k} N_{j,\beta_{n3}} \lhd H_k F_\tau F_s \rhd_{A_k} \\
& + C_{36}^{k} \lhd N_i N_{n3} \rhd_{\Omega_k} N_{j,\beta_{n3}} \lhd F_{\tau_{,z}} F_s \rhd_{A_k} \\
K_{32}^{k\tau sij} = {} & C_{22}^{k}\frac{1}{R_k}N_{i_{m2}} \lhd N_{m2}N_{n2} \rhd_{\Omega_k} N_{j,\beta_{n2}} \lhd H_k^2 F_\tau F_s \rhd_{A_k} \\
& + C_{23}^{k} \lhd N_i N_{n2} \rhd_{\Omega_k} N_{j,\beta_{n2}} \lhd H_k F_{\tau_{,z}} F_s \rhd_{A_k} \\
& + C_{26}^{k}\frac{1}{R_k}N_{i_{m2}} \lhd N_{m2}N_{n3} \rhd_{\Omega_k} N_{j,\alpha_{n3}} \lhd H_k^2 F_\tau F_s \rhd_{A_k} \\
& + C_{36}^{k} \lhd N_i N_{n3} \rhd_{\Omega_k} N_{j,\alpha_{n3}} \lhd H_k F_{\tau_{,z}} F_s \rhd_{A_k} \\
& - C_{45}^{k}\frac{1}{R_k}N_{i,\alpha_{m1}} \lhd N_{m1}N_{n2} \rhd_{\Omega_k} N_{j_{n2}} \lhd F_\tau F_s \rhd_{A_k} \qquad (4.40) \\
& - C_{44}^{k}\frac{1}{R_k}N_{i,\beta_{m2}} \lhd N_{m2}N_{n2} \rhd_{\Omega_k} N_{j_{n2}} \lhd F_\tau F_s \rhd_{A_k} \\
& + C_{45}^{k} N_{i,\alpha_{m1}} \lhd N_{m1}N_{n2} \rhd_{\Omega_k} N_{j_{n2}} \lhd H_k F_\tau F_{s_{,z}} \rhd_{A_k} \\
& + C_{44}^{k} N_{i,\beta_{m2}} \lhd N_{m2}N_{n2} \rhd_{\Omega_k} N_{j_{n2}} \lhd H_k F_\tau F_s \rhd_{A_k}
\end{aligned}
$$

$$
\begin{aligned}
K_{33}^{k\tau sij} = {} & C_{22}^{k} \frac{1}{R_k^2} N_{i_{m2}} \lhd N_{m2} N_{n2} \rhd_{\Omega_k} N_{j_{n2}} \lhd H_k^2 F_\tau F_s \rhd_{A_k} \\
& + C_{23}^{k} \frac{1}{R_k} N_{i_{m2}} \lhd N_{m2} N_j \rhd_{\Omega_k} \lhd H_k F_\tau F_{s_{,z}} \rhd_{A_k} \\
& + C_{23}^{k} \frac{1}{R_k} \lhd N_i N_{n2} \rhd_{\Omega_k} N_{j_{n2}} \lhd H_k F_{\tau_{,z}} F_s \rhd_{A_k} \\
& + C_{33}^{k} \lhd N_i N_j \rhd_{\Omega_k} \lhd F_{\tau_{,z}} F_{s_{,z}} \rhd_{A_k} \\
& + C_{55}^{k} N_{i,\alpha_{m1}} \lhd N_{m1} N_{n1} \rhd_{\Omega_k} N_{j,\alpha_{n1}} \lhd F_\tau F_s \rhd_{A_k} \\
& + C_{45}^{k} N_{i,\beta_{m2}} \lhd N_{m2} N_{n1} \rhd_{\Omega_k} N_{j,\alpha_{n1}} \lhd F_\tau F_s \rhd_{A_k} \\
& + C_{45}^{k} N_{i,\alpha_{m1}} \lhd N_{m1} N_{n2} \rhd_{\Omega_k} N_{j,\beta_{n2}} \lhd F_\tau F_s \rhd_{A_k} \\
& + C_{44}^{k} N_{i,\beta_{m2}} \lhd N_{m2} N_{n2} \rhd_{\Omega_k} N_{j,\beta_{n2}} \lhd F_\tau F_s \rhd_{A_k}
\end{aligned}
$$

where $\lhd \cdots \rhd_{\Omega_k}$ indicates $\int_{\Omega_k} \ldots d\Omega_k$ and $\lhd \cdots \rhd_{A^k}$ indicates $\int_{A_k} \ldots dz_k$.

### 4.9 Numerical Examples

The model introduced does not involve an approximation of the geometry of the shell and it accurately describes the curvature of the shell. However, the locking phenomenon is still present. In this work, the model is combined with a simple displacement formulation. The CUF, coupled with the MITC method, allows us to increase the degree of approximation by increasing the order of expansion of the displacements in the thickness direction and the number of elements used. Firstly, the reliability of the model is analyzed. Two classical discriminating test problems are considered: the pinched cylinder with a diaphragm [62], which is the most severe test for both inextensional bending modes and complex membrane states; and the Scordelis–Lo problem [63], which is extremely useful for determining the ability of a finite element to accurately solve complex states of a membrane strain.

The pinched shell has been analyzed in [32] and the essential shape is shown in Fig. 4.7. It is simply supported at each end by a rigid diaphragm and singularly loaded by two opposing forces acting at the midpoint of the shell. Due to the symmetry of the structure the computations have been performed, using a uniform decomposition, on an octave of the shell. The physical data given in Table 4.1 have been assumed. The following

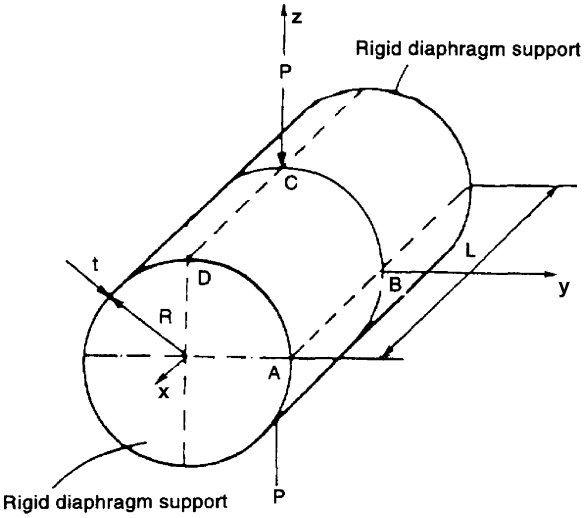


Fig. 4.7. Pinched shell.

Table 4.1. Physical data for pinched shell.

| | | |
|---|---|---|
| Young's modulus | $E$ | $3 \times 10^6$ psi $= 20.684 \times 10^9$ N/m$^2$ |
| Poisson's ratio | $\nu$ | 0.3 |
| Load | $P$ | 1 lb $= 0.154$ Kg |
| Length | $L$ | 600 in $= 15.24$ m |
| Radius | $R$ | 300 in $= 7.62$ m |
| Thickness | $h$ | 3 in $= 0.0762$ m |

symmetry conditions and boundary conditions are applied:

$$\begin{aligned} &v_s(\alpha, 0) = 0 \\ &u_s(0, \beta) = 0 \\ &v_s(\alpha, R\pi/2) = 0 \\ &v_s(L/2, \beta) = w_s(L/2, \beta) = 0 \end{aligned} \tag{4.41}$$

with $s = 0, 1, \ldots, N$.

In Table 4.2 the transversal displacement at the loaded point C is presented for several decompositions $[n \times n]$ and different theories. The high-order equivalent single-layer theories in the CUF are indicated with the acronym ESL$N$, where $N$ is the order of expansion. The exact solution is given by Flügge in [70] $1.8248 \times 10^{-5}$ in. The table shows that the MITC9

Table 4.2. Pinched shell. Transversal displacement $w$ in $\times 10^5$.

| Theory | $[4 \times 4]$ | $[10 \times 10]$ | $[13 \times 13]$ |
|---|---|---|---|
| Koiter | 1.7891 | 1.8231 | 1.8253 |
| Naghdi | 1.7984 | 1.8364 | 1.8398 |
| ESL1 | 1.9212 | 1.9583 | 1.9617 |
| ESL2 | 1.7805 | 1.8361 | 1.8408 |
| ESL3 | 1.7818 | 1.8380 | 1.8428 |
| ESL4 | 1.7818 | 1.8380 | 1.8428 |

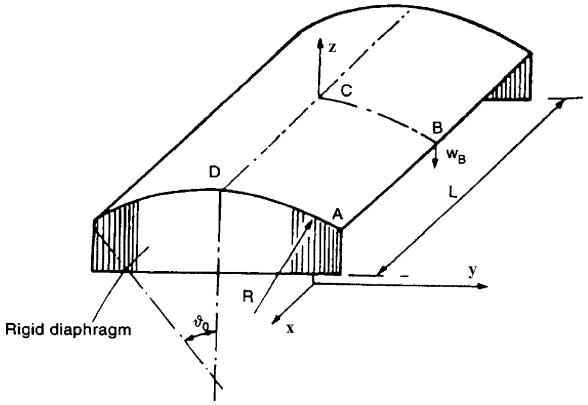


Fig. 4.8. Scordelis–Lo roof.

element has good convergence and robustness on increasing the mesh size. According to Reddy [21], the results obtained with high-order theories are greater than the reference value because Flügge uses a classical shell theory. Indeed, the solution calculated with the Koiter model for mesh $[13 \times 13]$ is very close to the exact solution, while the Naghdi model, which takes into account the shear energy, gives a higher value, as one would expect. The ESL theory with linear expansion (ESL1) produces such a high value because a correction for Poisson locking has been applied (for details of Poisson locking one can refer to [72]), but for cylindrical shell structures this correction causes problems. The remaining theories give almost the same results and they converge to the same value ($1.842 \times 10^{-5}$ in) by increasing the order of expansion and the number of elements used.

The second problem (the Scordelis–Lo problem [71]) concerns a cylindrical shell known in the literature as a barrel vault, see Fig. 4.8. The

Table 4.3. Physical data for barrel vault.

| | | |
|---|---|---|
| Young's modulus | $E$ | $4.32 \times 10^6$ lb/h$^2$ $= 20.684 \times 10^9$ N/m$^2$ |
| Poisson's ratio | $\nu$ | 0.0 |
| Load | $P$ | 90 lb/ft$^2$ $= 4309.224$ N/m$^2$ |
| Length | $L$ | 50 ft $= 15.24$ m |
| Radius | $R$ | 25 ft $= 7.62$ m |
| Thickness | $h$ | 0.25 ft $= 0.0762$ m |
| Angle | $\theta_0$ | $2\pi/9$ rad |

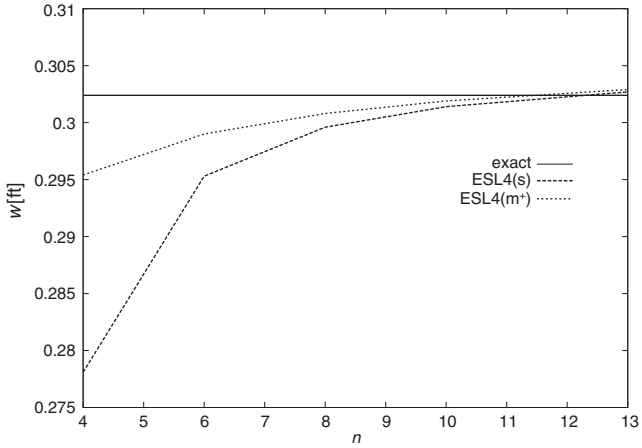


Fig. 4.9. Scordelis–Lo problem. Transversal displacement $w$ [ft] at the point B of the mid–surface $S$.

shell is simply supported on diaphragms, is free on its other sides, and is loaded by its own weight $P$. The physical data given in Table 4.3 have been assumed. The computations were performed only on a quarter of the shell, using a uniform decomposition.

The exact solution for this problem is given by McNeal and Harder in [73] in terms of the transversal displacement at the point B: 0.3024 ft. In Fig. 4.9, the solution is given for several decompositions $[n \times n]$. The performance of the MITC9 element in which a correction for both shear and membrane locking has been applied $(m^+)$ is compared with an element in which only shear locking has been corrected $(s)$. The figure confirms the conclusions for the pinched shell: the results converge to the exact solution on increasing the number of elements used. Moreover, the figure shows that for thin shells $(h/R = 0.01)$ the correction for membrane locking is essential because for coarse meshes the solution $(m^+)$ is much higher than the $(s)$

solution. One can conclude that the MITC9 element is completely locking free. The theory used for this analysis is ESL4 but the behavior is the same also for the other models.

Finally, a multilayered shell was analyzed in order to show the superiority of LW and the zig-zag models compared to ESL models. The orthotropic cylindrical shell studied by Varadan and Bhaskar in [74] is considered. The ends are simply supported. The loading is an internal sinusoidal pressure, applied normal to the shell surface, given by:

$$p_z^+ = \hat{p}_z^+ \sin\left(\frac{m\pi\alpha}{a}\right) \sin\left(\frac{n\pi\beta}{b}\right), \tag{4.42}$$

where the wave numbers are $m = 1$ and $n = 8$. The amplitude of the load $\hat{p}_z^+$ is assumed to be 1. $a$ is the length and $b$ the circumference of the cylinder.

The cylinder is made up of three equal layers with lamination $(90°/0°/90°)$. Each layer is assumed to be made of a square symmetric unidirectional fibrous composite material with the following properties:

$$\begin{aligned} &E_L/E_T = 25 \\ &G_{LT}/E_T = 0.5 \\ &G_{TT}/E_T = 0.2 \\ &\nu_{LT} = \nu_{TT} = 0.25, \end{aligned} \tag{4.43}$$

where $L$ is the direction parallel to the fibers and $T$ is the transverse direction. The length $a$ of the cylinder is assumed to be $4R_\beta$, and the radius $R_\beta$, referred to the mid-surface of the whole shell, is 10. Since the cylinder is a symmetric structure and it is symmetrically loaded, the computations were performed only on an octave of the shell, using a uniform decomposition.

The solution is given in terms of the transversal displacement $w$ for different values of the thickness ratio $R_\beta/h$, where $h$ is the global thickness of the cylinder. According to [74], the following dimensionless parameter is used:

$$\bar{w} = w\frac{10E_L h^3}{\hat{p}_z^+ R_\beta^4}. \tag{4.44}$$

The results are presented in Table 4.4 and are compared with the 3D-elasticity solution given by Varadan and Bhaskar in [74]. The transversal

Table 4.4. Varadan and Bhaskar. Dimensionless transversal displacement at the max-loading point in $z = 0$.

| $R_\beta/h$ | 2 | 4 | 10 | 50 | 100 | 500 |
|---|---|---|---|---|---|---|
| 3D | 10.1 | 4.009 | 1.223 | 0.5495 | 0.4715 | 0.1027 |
| ESL4 | 9.682 | 3.782 | 1.1438 | 0.5456 | 0.4707 | 0.1029 |
| ESL3 | 9.664 | 3.785 | 1.1439 | 0.5456 | 0.4707 | 0.1029 |
| ESL2 | 8.280 | 2.971 | 0.9540 | 0.5378 | 0.4692 | 0.1029 |
| ESL1 | 8.925 | 3.015 | 0.9559 | 0.5380 | 0.4696 | 0.1034 |
| Naghdi | 8.421 | 2.872 | 0.9382 | 0.5370 | 0.4688 | 0.1029 |
| Koiter | 0.4094 | 0.4796 | 0.5205 | 0.5209 | 0.4656 | 0.1029 |
| ESLZ3 | 9.791 | 3.987 | 1.224 | 0.5493 | 0.4715 | 0.1029 |
| ESLZ2 | 9.596 | 3.866 | 1.191 | 0.5479 | 0.4712 | 0.1029 |
| ESLZ1 | 10.228 | 3.901 | 1.191 | 0.5457 | 0.4694 | 0.1028 |
| LW4 | 10.267 | 4.032 | 1.225 | 0.5493 | 0.4715 | 0.1029 |
| LW3 | 10.256 | 4.031 | 1.225 | 0.5493 | 0.4715 | 0.1029 |
| LW2 | 9.789 | 3.971 | 1.223 | 0.5493 | 0.4715 | 0.1029 |
| LW1 | 9.689 | 3.874 | 1.191 | 0.5477 | 0.4710 | 0.1029 |

displacement is calculated on the mid-surface of the multilayered shell ($z = 0$), at the max-loading point. An $[8 \times 8]$ mesh was used, which is sufficient to ensure numerical convergence. Equivalent single-layer (ESL$N$), zig-zag (ESLZ$N$), and layer-wise (LW$N$) theories in the CUF are employed for the analysis. Also the classical Koiter's and Naghdi's models were used for comparison. One can note that the solution obtained with the classical models is completely wrong, while the ESL theories give a more accurate solution by increasing the order of expansion $N$, especially for high-thickness ratios. If one takes into account also the zig-zag effects in the displacements using Murakami's zig-zag function (ESLZ models), the results improve again and the ESLZ3 theory provides approximately the 3D solution even for very thick shells. Finally, the table shows that the LW theories give the best results even when the order of expansion is not high ($N$ = 2,3), according to the assertions made in the introduction of this chapter about $C_z^0$-requirements. This behavior is particularly visible for thick shells ($R_\beta/h = 2, 4$). For very thin shells ($R_\beta/h = 500$) all the theories converge to the 3D solution and this fact demonstrates once again the numerical efficiency of the new approach. Note that the LW3 and LW4 models give a solution slightly higher than the 3D solution for very thick shells. This is due to a curvature approximation along the thickness, which can be easily eliminated by considering the shell to be composed of thinner fictitious layers with the same properties.

### 4.10 Conclusions

In this chapter, it has been shown that there are three independent ways of introducing "zig-zag" theories for the analysis of multilayered plates and shells. In particular, it has been established that:

- Lekhnitskii [22] was the first to propose a theory for multilayered structures that describes the zig–zag form of a displacement field in the thickness direction and the interlaminar equilibrium of transverse stresses.
- Three different and independent theories are proposed in the literature. Apart from the one by Lekhnitskii [22], the other two approaches were based on work by Ambartsumian [44, 55] and Reissner [48], respectively.
- Based on the authors' historical considerations, which are documented in this chapter, it is suggested that these three approaches are called the Lekhnitskii–Ren, Ambartsumian–Whitney–Rath–Das, and Reissner–Murakami–Carrera theories, respectively.
- As far as the Ambartsumian–Whitney–Rath–Das theory is concerned, it should be underlined that other developments, even though derived independently by other authors (such as those originated by Yu [75] and Chou and Carleone [76], Disciuva [77], Bhaskar and Varadan [78], Cho and Parmerter [79], among others), are applications of the AWRD theory.

Even though most of this discussion has been about the so-called ESLMs, these being more relevant for the subject of this chapter, a brief outline of LWMs was given in Section 4.7.

The author would encourage scientists, who are working on the analysis of multilayer structures, to return to the fundamental work by Lekhnitskii [22], Ambartsumian [44, 45], and Reissner [48]. There is, in fact, a significant amount to learn from these works and probably more could be done, on the basis of these fundamental works, to obtain a better understanding of the mechanics of multilayered structures. In particular, future developments could be to extend Lekhnitskii's theory as well as Reissner's theorem. This latter, in the authors' opinion, is the natural tool for the analysis of multilayered structures.

As a final remarks the authors are clearly aware that this historical review may be not complete. The authors are aware that other significant articles and papers could exist on this subject that have not been considered. However, what has been quoted in this chapter will help to

assign the right credit concerning the contributions and contributors to multilayered theory.

The final part of this chapter discussed the development of a refined shell finite element approach based on Carrera's unified formulation. The CUF has been coupled to the MITC method to overcome the locking phenomenon that affects finite element analysis. The reliability of the approach has been tested by considering classical discriminating problems, such as the pinched cylinder studied in [70] and the Scordelis–Lo problem analyzed in [71], and the approach has shown good convergence and robustness on growing the mesh size. Moreover, the accuracy of the solution has been demonstrated to improve by increasing the order of expansion of the displacements in the thickness direction. Finally, the orthotropic multilayered cylinder studied by Varadan and Bhaskar in [74] was considered. From this analysis one can conclude that for the study of multilayered structures it is mandatory to consider zig-zag effects in the displacements in order to obtain the 3D solution. This is possible by introducing Murakami's zig-zag function in the ESL models or by using the LW models briefly discussed in this chapter, which allow us to use independent variables in each layer. This gives the best results.

For clarity, Table 4.5 summarizes the features of the theories cited in this chapter for the analysis of laminated structures:

- Classical = classical models such as Kirchoff–Love, Reissner–Mindlin, and so on;
- CUF-ESL = equivalent single-layer theories contained in the CUF, in which a high order of expansion in the thickness direction is used for both the in-plane and ransversal displacements;
- L = Lekhnitskii theory;
- LR = Lekhnitskii–Ren theory;

Table 4.5. Available theories for laminated structures.

| Theory | $\sigma_{nM}$ | ZZ | IC | $\epsilon_{zz}$ | $\sigma_{zz}$ |
|---|---|---|---|---|---|
| Classical [1–6] | | | | | |
| CUF-ESL [9, 27] | | | | • | • |
| L [22] | | • | • | • | |
| LR [38–40] | | • | • | | |
| AWRD [41–46] | | • | • | | |
| RMC [47–53] | • | • | • | • | • |
| CUF-LW-D [60] | | • | | • | • |
| CUF-LW-M [54–60] | • | • | • | • | • |

- AWRD = Ambartsumian–Whitney–Rath–Das theory;
- RMC = Reissner–Murakami–Carrera theory, based on ESL approach for displacement variables;
- CUF-LW-D = layer-wise models contained in the CUF, based on the principle of virtual displacements (PVD);
- CUF-LW-M = layer-wise models contained in the CUF, based on the Reissner mixed variational theorem (RMVT).

The features, considered in the table, are the following:

- $\sigma_{nM}$ = the transverse shear and normal stresses are unknown variables with the displacements;
- ZZ = zig-zag effects are considered in the displacements;
- IC = interlaminar continuity of the transverse stresses is fulfilled;
- $\epsilon_{zz}$ = thickness stretching effects are considered, $\epsilon_{zz} \neq 0$;
- $\sigma_{zz}$ = Koiter's recommendation is fulfilled, $\sigma_{zz} \neq 0$.

The symbol • indicates that the theory satisfies the corresponding feature.

## References

[1] Cauchy A.L., 1828. Sur l'équilibre et le mouvement d'une plaque solide, *Exercises de Matematique*, 3, 328–355.
[2] Poisson S.D., 1829. Mémoire sur l'équilibre et le mouvement des corps élastique, *Mem. Acad. Sci.*, 8, 357.
[3] Kirchhoff G., 1850. Über das Gleichgewicht und die Bewegung einer elastishen Scheibe, *J. Angew. Math.*, 40, 51–88.
[4] Love A.E.H., 1927. *The Mathematical Theory of Elasticity*, 4th edn., Cambridge University Press, Cambridge.
[5] Reissner E., 1945. The effect of transverse shear deformation on the bending of elastic plates, *J. Appl. Mech.*, 12, 69–76.
[6] Mindlin R.D., 1951. Influence of rotatory inertia and shear in flexural motions of isotropic elastic plates, *J. Appl. Mech.*, 18, 1031–1036.
[7] Hildebrand F.B., Reissner E., Thomas G.B., 1938. Notes on the foundations of the theory of small displacements of orthotropic shells. NACA TN-1833, Washington, DC.
[8] Pagano N.J., 1969. Exact solutions for composite laminates in cylindrical bending, *J. Compos. Mater.*, 3, 398–411.
[9] Carrera E., 1995. A class of two dimensional theories for multilayered plates analysis, *Atti Accademia delle Scienze di Torino, Mem Sci. Fis.*, 19–20, 49–87.
[10] Ambartsumian S.A., 1962. Contributions to the theory of anisotropic layered shells, *Appl. Mech. Rev.*, 15, 245–249.

[11] Librescu L., Reddy J.N., 1986. A critical review and generalization of transverse shear deformable anisotropic plates, *Euromech Colloquium 219, Refined dynamical theories of beams, plates and shells and their applications*, Kassel, September, 32–43.
[12] Grigolyuk E.I., Kulikov G.M., 1988. General directions of the development of theory of shells, *Mekhanica Kompozitnykh Materialov*, 24, 287–298.
[13] Kapania R.K., Raciti S., 1989. Recent advances in analysis of laminated beams and plates, *AIAA J.*, 27, 923–946.
[14] Kapania R.K., 1989. A review on the analysis of laminated shells, *J. Press. Vess. Tech.*, 111, 88–96.
[15] Noor A.K., Burton W.S., 1989. Assessment of shear deformation theories for multilayered composite plates, *Appl. Mech. Rev.*, 41, 1–18.
[16] Noor A.K., Burton W.S., 1990. Assessment of computational models for multilayered composite shells, *Appl. Mech. Rev.*, 43, 67–97.
[17] Noor A.K., Burton W.S., Bert C.W., 1996. Computational model for sandwich panels and shells, *Appl. Mech. Rev.*, 49, 155–199.
[18] Reddy J.N., Robbins D.H., 1994. Theories and computational models for composite laminates, *Appl. Mech. Rev.*, 47, 147–165.
[19] Carrera E., 2001. Developments, ideas and evaluations based upon the Reissner's Mixed Theorem in the modeling of multilayered plates and shells, *Appl. Mech. Rev.*, 54(4), 301–329.
[20] Librescu L., 1975. *Elasto-Statics and Kinetics of Anisotropic and Heterogeneous Shell-type Structures*, Noordhoff Int., Leyden, Netherlands.
[21] Reddy J.N., 1997. *Mechanics of Laminated Composite Plates, Theory and Analysis*, CRC Press, Boca Raton.
[22] Lekhnitskii S.G., 1935. Strength calculation of composite beams, *Vestn. Inzh. Tekh.*, 9.
[23] Carrera E., 2003. Historical review of zig-zag theories for multilayered plates and shells, *Appl. Mech. Rev.*, 56(3), 287–308.
[24] Fettahlioglu O.A., Steele C.R., 1974. Asymptotic solutions for orthotropic non-homogeneous shells of revolution, *J. Appl. Mech.*, 41(3), 753–758.
[25] Hodges D.H., Lee B.W., Atilgan A.R., 1993. Application of the variational-asymptotic method to laminated composite plates, *AIAA J.*, 31, 1674–1983.
[26] Satyrin V.G., Hodges D.H., 1996. On asymptotically correct linear laminated plate theory, *Int. J. Solids Struct.*, 33, 3649–3671.
[27] Carrera E., 2003. Theories and finite elements for multilayered plates and shells: a unified compact formulation with numerical assessment and benchmarking, *Arch. Comput. Meth. Eng.*, 97, 10–215.
[28] Carrera E., 1999. Transverse normal stress effects in multilayered plates, *J. Appl. Mech.*, 66, 1004–1012.
[29] Koiter W.T., 1970. On the foundations of the linear theory of thin elastic shell, *Proc. Kon. Nederl. Akad. Wetensch.*, 73, 169–195.
[30] Naghdi P.M., 1972. The theory of shells and plates, *Handbuch der Physik.*, 6, 425–640.

[31] Hakula H., Leino Y., Pitkäranta J., 1996. Scale resolution, locking, and higher-order finite element modelling of shells, *Comp. Meth. Appl. Mech. Eng.*, 133, 155–182.
[32] Chinosi C., Della Croce L., Scapolla T., 1998. Hierarchic finite elements for thin Naghdi shell model, *Int. J. Solids Struct.*, 35, 1863–1880.
[33] Zienkiewicz O.C., Taylor R.L., Too J.M., 1971. Reduced integration techniques in general analysis of plates and shells, *Int. J. Num. Meth. Eng.*, 3, 275–290.
[34] Stolarski H., Belytschko T., 1981. Reduced integration for shallow-shell facet elements, in *New Concepts in Finite Element Analysis* (T.J.R. Hughes, *et al.*, eds), ASME, New York, pp. 179–194.
[35] Bathe K.-J., Dvorkin E., 1986. A formulation of general shell elements the use of mixed interpolation of tensorial components, *Int. J. Num. Meth. Eng.*, 22, 697–722.
[36] Chinosi C., Della Croce L., 1998. Mixed-interpolated elements for thin shell, *Comm. Num. Meth. Eng.*, 14, 1155–1170.
[37] Huang H.-C., 1987. Membrane locking and assumed strain shell elements, *Comp. Struct.*, 27(5), 671–677.
[38] Lekhnitskii S.G., 1968. *Anisotropic Plates*, translated from the 2nd Russian edn by S.W. Tsai and T. Cheron, Bordon and Breach, Science Publishers, New York.
[39] Ren J.G., 1986. A new theory of laminated plates, *Compos. Sci. Tech.*, 26, 225–239.
[40] Ren J.G., 1986. Bending theory of laminated plates, *Compos. Sci. Tech.,* 27, 225–248.
[41] Ren J.G., D.R. Owen J., 1989. Vibration and buckling of laminated plates, *Int. J. Solids Struct.*, 25, 95–106.
[42] Ambartsumian S.A., 1958. On a theory of bending of anisotropic plates, *Investiia Akad. Nauk. SSSR, Ot. Tekh. Nauk.*, No. 4.
[43] Ambartsumian S.A., 1958. On a general theory of anisotropic shells, *Prikl. Mat. Mekh.*, 22(2), 226–237.
[44] Ambartsumian S.A., 1961. Theory of anisotropic shells, *Fizmatgiz, Moskwa*, translated from Russian, NASA TTF–118.
[45] Ambartsumian S.A., 1969. *Theory of Anisotropic Plates*, translated from Russian by T. Cheron and edited by J.E. Ashton, Technomic Pub. Co.
[46] Whitney J.M., 1969. The effects of transverse shear deformation on the bending of laminated plates, *J. Compos. Mater.*, 3, 534–547.
[47] Rath B.K., Das Y.C., 1973. Vibration of layered shells, *J. Sound Vib.*, 28, 737–757.
[48] Reissner E., 1984. On a certain mixed variational theory and a proposed application, *Int. J. Num. Meth. Eng.*, 20, 1366–1368.
[49] Reissner E., 1986. On a mixed variational theorem and on a shear deformable plate theory, *Int. J. Num. Meth. Eng.*, 23, 193–198.
[50] Murakami H., 1985. Laminated composite plate theory with improved in-plane responses, *ASME Proceedings of PVP Conference*, New Orleans, June 24–26, 98(2), 257–263.

[51] Murakami H., 1986. Laminated composite plate theory with improved in-plane response, *J. Appl. Mech.*, 53, 661–666.
[52] Carrera E., 1999. A study of transverse normal stress effects on vibration of multilayered plates and shells, *J. Sound Vib.*, 225, 803–829.
[53] Toledano A., Murakami H., 1987. A high-order laminated plate theory with improved in-plane responses, *Int. J. Sol. Struct.*, 23, 111–131.
[54] Carrera E., 1997. An improved Reissner-Mindlin-Type model for the electromechanical analysis of multilayered plates including piezo-layers, *J. Intel. Mat. Syst. Struct.*, 8, 232–248.
[55] Carrera E., 1998. Evaluation of layer-wise mixed theories for laminated plates analysis, *AIAA J.*, 36, 830–839.
[56] Carrera E., 1998. Layer-wise mixed models for accurate vibration analysis of multilayered plates, *J. Appl. Mech.*, 65, 820–828.
[57] Carrera E., 1999. A Reissner's mixed variational theorem applied to vibrational analysis of multilayered shell, *J. Appl. Mech.*, 66(1), 69–78.
[58] Carrera E., 1999. Transverse normal stress effects in multilayered plates, *J. Appl. Mech.*, 66, 1004–1012.
[59] Carrera E., 2000. Single-layer vs multi-layers plate modelings on the basis of Reissner's mixed theorem, *AIAA J.*, 38, 342–343.
[60] Carrera E., 2000. *A priori* vs *a posteriori* evaluation of transverse stresses in multilayered orthotropic plates, *Compos. Struct.*, 48, 245–260.
[61] Bhaskar K., Varadan T.K., 1992. Reissner's new mixed variational principle applied to laminated cylindrical shells, *J. Press. Vessel Tech.*, 114, 115–119.
[62] Jing H., Tzeng K.G., 1993. Refined shear deformation theory of laminated shells, *AIAA J.*, 31, 765–773.
[63] Rao K.M., Meyer-Piening H.R., 1990. Analysis of thick laminated anisotropic composites plates by the finite element method, *Compos. Struct.*, 15, 185–213.
[64] Carrera E., 1996. $C^0$ Reissner-Mindlin multilayered plate elements including zigzag and interlaminar stresses continuity, *Int. J. Num. Meth. Eng.*, 39, 1797–1820.
[65] Carrera E., Kröplin B., 1997. Zig-zag and interlaminar equilibria effects in large deflection and postbuckling analysis of multilayered plates, *Mech. Compos. Mat. Struct.*, 4, 69–94.
[66] Bhaskar K., Varadan T.K., 1991. A higher-order theory for bending analysis of laminated shells of revolution, *Comp. Struct.*, 40, 815–819.
[67] Brank B., Carrera E., 2000. Multilayered shell finite element with interlaminar continuous shear stresses: a refinement of the Reissner-Mindlin formulation, *Int. J. Num. Meth. Eng.*, 48, 843–874.
[68] Cho Y.B., Averill R.C., 2000. First order zig-zag sub-laminate plate theory and finite element model for laminated composite and sandwich panels, *Comp. Struct.*, 50, 1–15.
[69] Chapelle D., Bathe K.-J., 2003. *The Finite Element Analysis of Shells. Fundamentals*, Springer, Berlin.
[70] Flügge W., 1960. *Stresses in Shells*, 2nd edn, Springer, Berlin.

[71] Scordelis A., Lo K.S., 1964. Computer analysis in cylindrical shells, *J. Amer. Concr. Inst.*, 61, 561–593.
[72] Carrera E., Brischetto S., 2008. Analysis of thickness locking in classical, refined and mixed theories for layered shells, *Compos. Struct.*, 85(1), 83–90.
[73] McNeal R.H., Harder R.L., 1985. A proposed standard set of problems to test finite element accuracy, *Fin. Elem. in Anal. Des.*, 1, 3–20.
[74] Varadan T.K., Bhaskar K., 1991. Bending of laminated orthotropic cylindrical shells — an elasticity approach, *Compos. Struct.*, 17, 141–156.
[75] Yu Y.Y., 1959. A new theory of elastic sandwich plates one dimensional case, *J. Appl. Mech.*, 37, 1031–1036.
[76] Chou P.C., Carleone J., 1973. Transverse shear in laminated plates theories, *AIAA J.*, 11, 1333–1336.
[77] Disciuva M., 1984. A refinement of the transverse shear deformation theory for multilayered plates, *Aerotecnica Missili e Spazio*, 63, 84–92.
[78] Bhaskar B., Varadan T.K., 1989. Refinement of higher-order laminated plate theories, *AIAA J.*, 27, 1830–1831.
[79] Cho M., Parmerter R.R., 1993. Efficient higher order composite plate theory for general lamination configurations, *AIAA J.*, 31, 1299–1305.